Some Observations on Trace and Ree Geochemistry of Magnetites of Domna Pahari, Palamu District, Jharkhand.

Krishna Gopal[1]

[1]*DST(GOI)- INSPIRE Fellow, University Department of Geology, Ranchi University, Ranchi-834008*

Abstract: The magnetite deposits of Domna Pahari, located southwest of Medninagar town in Palamu district of Jharkhand occur associated with metaultramafites in the form of concordant bands, pockets, lenses and disseminations. The deposit is both structurally and lithologically controlled under the microscope magnetite is present as the major constituent with minor amount of hematite, goethite and martite. Calc silicate minerals typical of skarn deposits are absent. The concentration of Cu, P, Ti, Cr and V as well as Co/Ni, Cr/V, LREE/HREE, Eu/Sm, Sm/Yb, La/Lu of the studied magnetite ores indicate that they are of hydrothermal magnetite type. Geochemical plots show that the host rock is iron rich thoeliite which may acted as source of iron and heat in the mineralizing system.

Key words: Chotanagpur Gneissic Complex, Magnetite, Domna Pahari, Trace and REE, Hydrothermal deposit.

I. INTRODUCTION

The majority of magnetite ore deposits of magmatic or magmatic-hydrothermal association are found in rocks of Early to middle Proterozoic age (1.8-1.1 Ga). The formation mechanism of magnetite deposits of magmatic association has been the subject of much controversy. A wide range of geological processes have been suggested for formation of magnetite deposits such as by (a) hydrothermal processes (b)magmatic intrusion (c) liquid immiscibility of an iron-rich melt (d)volcanic- sedimentary exhalative processes and (e) remobilization of older, iron and phosphorous- rich sedimentary rocks.

In general, at lower temperature magnetite concentrates to form hydrothermal deposits and at high temperature it crystallizes together with silicate- sulphide minerals from primary magmatic melts. Magnetite compositions can reveal the physicochemical conditions under which it was formed. Trace elements commonly present within the magnetite structure include Mg, Al, Sc, Ti, V, Cr, Mn, Co, Ni, Zn, Ga, Ge, Y, Hf, Nb, Mo, Ta and Zr in addition to Fe (Nadoll et al., 2012; Dare et al., 2014) Incorporation of trace elements within the magnetite depends on many factors including similarities of the ionic radius and cation valences, oxygen fugacity(fO2), magma/ fluid composition and temperature (Nadoll et al. 2014; Chen et al., 2015). In view of the above assumptions, the magnetite compositions vary in different ore forming environments. The present paper focuses on chemistry of magnetite ores and associated rocks occurring in Domna Pahari (N 240 0'50.0": E 830 56'03.7") the northwestern fringe of Chotanagpur Gneissic Complex(CGC) near Medninagar and an attempt has been made to postulate the genesis of the ore.

II. GEOLOGICAL SETUP

The area under investigation falls in the northwestern fringe of CGC which is a vast (80,000 Km2) ENE-WSW high grade terrane in the eastern part of Central Indian Tectonic Zone (CITZ, Fig.1). The structural trend of CGC is parallel to that of Satpura belt of Central India and a major gravity high extending from the western part of Satpura mountains in the west through Central India to the northern parts of the Damodar Graben in CGC (Verma 1985) indicates the continuity of two terranes. Sharma (2009) considers the CGC basement an isolated cratonic block and distinguishes it from the Satpura Fold belt that has the characteristics of a mobile belt. The gneissic basement and the supracrustals were affected by three deformation episodes (Patel et al., 2007)

The study area, situated near Medninagar in northwestern extreme of CGC, consists rocks belonging to amphibolites to granulite facies. These high grade rocks contain concordant, lenticular supracrustal enclaves and calc- silicates intruded by mafic-ultramafic rocks associated with magnetite deposits. Late intrusive non foliated granitoids cut across the basement gneisses and the supracrustals.

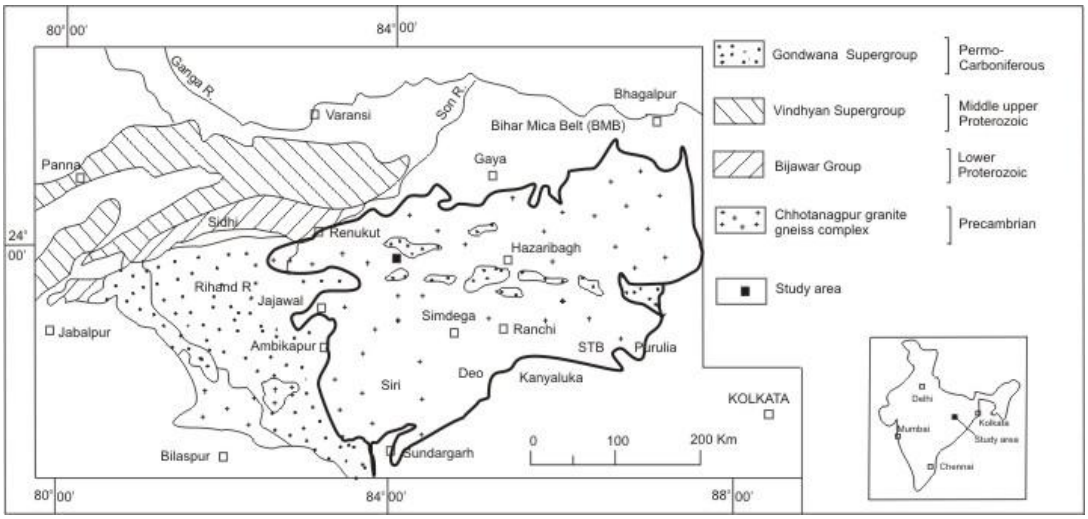

III. MODE OF OCCURRENCE

Magnetite in study area occur as pockets, concordant bands, lenses and disseminations mainly within tremolite actinolite schists and occasionally within chlorite schist, serpentinite and amphibolites. Their attitude is parallel to the regional foliation striking NW-SE in general having steep dip of 600 to 800 in NE direction. Extension of each pocket ranges from 30m to more than 80m in length and 5m to more than 16m in width. Magnetite near the wall rock shows laminations and are highly friable whereas away from the wall rocks, it is massive, very hard and compact. Innumerable tension cracks at high angle to almost vertical have been observed. However, at places, horizontal joints are also noticed.

IV. CONTROLS OF MINERALISATION

The magnetite mineralization of the area is controlled by both lithology and structure of the associated rocks . The different controls of mineralization are described below.

4.1 Lithological controls

The magnetite lode is confined to ultramafites which underwent regional metamorphism and now represented by tremolite actinolite schist, chlorite schist and serpentine rocks.

4.2 Structural controls

From the field and microscopic studies, it is evident that the structural features are the most important locii of mineralization of the ore bodies. The mineralization is conformable to the regional structure having in general NW-SE foliation. Subsequent folding and refolding have changed its attitude accordingly. Local variations have been marked at several places having almost NS extension. The discontinuous bands of chlorite schist and tremolite actinolite schist are folded giving rise to axial plane schistosity. These schistosity planes are produced due to first generation folds F. The magnetite mineralization is confined mainly along the schistosity plane clearly evidenced in field and microscopic studies. The regional plunge direction of the fold axis of first generation F has controlled the mineralization upto great extent.

V. PETROGRAPHY

Microscopically magnetite is present as major phase with subordinate amount of hematite, martite goethite and gangue minerals. Two generations of magnetite are observed. The first generation appears as fine grained magnetite with a granular texture. This early formed magnetite occurs commonly as euhedral crystals in crystal aggregates. This stage of the iron mineralization follows silicification. The second generation of magnetite have a coarse-grained massive texture, formed during recrystallization of first crystals. This magnetite is accompanied by a second generation of silica, indicating that the composition and/ or physical condition of the mineralizing fluid has changed under the microscope, perfect crystals of hematite can rarely be seen. Magnetite commonly oxidizes to hematite. Goethite mostly appears along grain boundaries and fractures replacing hematite and magnetite. Martitization is common in the studied ores. Martite replaces magnetite on grain boundaries and cleavage planes of the host mineral in oxidation zones. Rare sulfide including pyrite and chalcopyrite are observed as disseminated grains during

microscopic investigation. Sulphide formation post-dates the oxides. The microscopic replacement textures include remnant islands of the nonreplaced host mineral, replacement textures as a result of oxidation and hydrothermal alteration. At least three generation of quartz were detected in petrographic studies. The first generation occurred during silicification of the host prior to the magnetite formation. The second generation of quartz is characterized by orthomorphic medium sized quartz that shows inter-fingering border with magnetite. This quartz formed simultaneously with magnetite. The third generation of quartz occurs as veinlets that have cut the previously existing mineral. This generation constitutes veins that cut the whole ore body at a large scale. The activity of silica-rich hydrothermal fluid resulted in the formation of large veins of quartz as a final stage of fluid circulation.
Calc-silicate such as wollastonite and diopside, minerals typical of skarns, are virtually absent from the ore.

VI. GEOCHEMISTRY

10 nos. of representative samples of magnetite and 3 nos. of representative samples of host rock were analysed for major oxide, trace and rare earth elements at National Geophysical Research Institute (NGRI), Hyderabad. Major elements were determined by X-Ray Fluorescence Spectrophotometry (XRF) using Phillips MAGI X PRO model 2440.
The Trace and rare earth elements were analysed using magnetic sector High Resolution Inductively Coupled Plasma Mass Spectrometry (HR-ICP-MS). The precisiors obtained were <2% RSD for majority of elements with comparable accuracy (Satyanarayanan et al., 2018). The results of the analyses are tabulated in Table 1 to 6.

Table.1: Major Oxide (in wt%) of magnetite ores of Domna Pahari, Palamu district, Jharkhand.

Sample no.	KA4	KA2	KA1	KA3	KA6	KA7	KA5	KA9	KA8	KA10
SiO2	12.4	4.02	2.83	9.03	4.03	5.55	20.6	20.2	3.35	8.03
Al2O3	0.6	0.16	0.16	0.09	0.18	0.41	0.2	0.4	0.07	0.44
Fe2O3	61.3	63.1	70.4	59.1	73.2	63.4	62	53.3	71.6	51.3
MgO	1.9	3.1	1.2	1.1	1.2	2.1	1.7	3.1	0.9	1.5
MnO	3.95	0.31	0.37	0.13	0.85	4.2	4.17	5.31	0.003	0.15
CaO	0.019	0.004	0.009	0.135	0.03	0.006	0.007	0.167	0.004	0.029
Na2O	0.9	1.21	0.94	0.95	0.99	1.04	0.98	0.95	1.09	1.01
K2O	0.08	0.01	0.06	0.07	0.05	0.11	0.07	0.12	0.03	0.06
P2O5	0.0004	0.0035	0.0002	0.0056	0.009	0.0066	0.0065	0.0065	0.0063	0.0091
LOI	10.02	10.6	9.85	9.35	12.6	7.65	5.55	12.6	14.8	19.02

Table.2:Trace Elements (in ppm) of magnetite ores of Domna Pahari, Palamu district, Jharkhand.

	KA4	KA2	KA1	KA3	KA6	KA7	KA5	KA9	KA8	KA10
Co	16.1	42.2	46	51	21.3	29	59.1	23.2	33.9	7.8
Ni	3	9	4	12	4	6	9	16	26	9
Cu	905	4100	4	76	43	17	50	11	20	4
Zr	4.9	1.9	1.2	1.2	1.9	1.9	2.5	6.2	3.5	3.6
Sr	237	875	467	88	626	38	28	408	436	376
Zn	12	23	31	16	39	21	9	57	26	136
Ba	36995	97150	1487	21488	2097	3566	666	1247	20297	17996
Cr	99	96	98	97	99	98	97	99	98	97
Ti	96	98	98	99	97	99	97	97	98	98
Ga	1	8	6	2	5	1	1	5	2	2
V	8	5	5	4	7	4	7	13	14	11
Cr/V	12.375	19.2	19.6	24.25	14.14	24.4	13.85	33	7	8.818
Co/Ni	5.366	4.688	11.5	4.25	0.325	4.83	6.566	0.2	1.303	0.8

Table.3: REE (in ppm)concentration of magnetite ores of Domna Pahari, Palamu district, Jharkhand.

	KA4	KA2	KA1	KA3	KA6	KA7	KA5	KA9	KA8	KA10
La	2.4	13.1	11.2	2.5	3.8	5.6	3.2	4.2	4.8	4.3
Ce	3.4	25	21.3	3.3	4.2	9.3	4.2	8.1	6.2	8.1
Pr	0.42	2.55	3.06	0.41	0.58	1.06	0.51	1.08	1.02	2.63

Nd	2.6	15.5	11.2	4.3	2.2	5.6	3.3	3.1	4.1	3.4
Sm	0.9	3.8	2.6	0.6	0.6	3.4	0.8	2.4	1.4	1.6
Eu	0.27	0.35	0.25	0.49	0.23	0.39	0.53	0.29	0.45	0.31
Gd	0.78	4.14	1.62	0.96	0.91	1.95	1.17	1.41	2.66	2.32
Tb	0.13	0.66	0.29	0.17	0.1	0.36	0.15	0.19	0.28	0.15
Dy	0.9	1.31	1.26	0.59	0.56	1.32	0.64	1.07	0.96	0.93
Ho	0.18	0.41	0.13	0.1	0.3	0.19	0.09	0.15	0.16	0.14
Er	0.45	1.02	0.32	0.36	0.27	0.62	0.25	0.42	0.46	0.39
Tm	0.04	0.13	0.05	0.04	0.04	0.06	0.04	0.04	0.04	0.04
Yb	0.1	0.5	0.2	0.3	0.3	0.2	0.1	0.1	0.3	0.1
Lu	0.06	0.08	0.04	0.04	0.05	0.12	0.05	0.05	0.05	0.04

Table.4:Major Oxide (in wt%) of host rocks of Domna Pahari, Palamu District, Jharkhand.

	KA4	KA2	KA1	KA3	KA6	KA7	KA5	KA9	KA8	KA10
SiO2	44.3	44.1	43.98	44.7	43.78	44.6	44.78	44.8	43.6	44.5
Al2O3	16.6	17.1	16.4	16.5	17.3	14.1	13.6	14.2	16.3	17.2
Fe2O3	12.59	13.22	12.01	13.32	12.75	13.6	14.1	13.2	12.02	13.19
MgO	9.9	9.6	9.2	9.8	9.3	9.7	9.4	9.24	9.32	9.26
MnO	0.016	0.015	0.001	0.017	0.016	0.17	0.3	0.26	0.002	0.014
CaO	11.6	11.22	10.65	10.92	11.96	7.9	6.5	7.61	10.62	11.2
Na2O	3.85	3.95	4.15	3.95	4.04	4.1	3.3	3.5	4.11	3.92
K2O	1.6	1.32	1.67	1.36	1.42	1.12	1.46	1.35	1.56	1.3
P2O5	0.27	0.258	0.23	0.242	0.248	0.22	0.29	0.28	0.232	0.256
SiO2	1.08	1.37	1.36	1.27	1.16	1.12	3.2	4.01	1.36	1.33

Table. 5: Trace Elements (in ppm) of host rocks of Domna Pahari, Palamu District, Jharkhand.

	KA4	KA7	KA9
Co	72	41.3	39.5
Ni	41	23	24
Cu	59	68	15
Zr	183	172	177
Sr	221	179	248
Zn	76	98	99
Ba	301	339	269
U	0.98	2.01	1.6
V	314	323	324
Ag	1	1	1
Y	33.1	36.2	36.1
Cr	100	100	102
Ti	10810	16885	22309
Ga	21	21	20

Table.6: REE (in ppm) concentration of host rocks of Domna Pahari, Palamu District, Jharkhand.

La	21.5	18.2	16.2
Ce	42.2	38.4	36.1
Pr	5.49	5.06	4.74
Nd	23.6	22.2	21.6
Sm	5.4	5.4	5.1
Eu	1.69	1.92	1.92
Gd	6.8	6.2	6.2

Tb	0.1	1.03	1.02
Dy	6.42	6.45	6.42
Ho	1.22	1.25	1.25
Er	4.08	4.11	4.04
Tm	0.052	0.51	0.52
Yb	3.2	3.1	3.1
Lu	0.49	0.47	0.45

The Fe2O3 content of ore bodies varies widely from 51.3 wt% to 73.2 wt% . The average content of MnO in the iron ore is moderately high (avg 1.944 wt%) but P2O5 is typically low (avg 0.005 wt%). The K2O and Na2O values of the iron ore samples are in the range of 0.01- 0.11 wt% and 0.90- 1.21 wt% respectively. The concentration of trace metals in the studied ores is very low e.g Co (7.2 to 59.1 ppm), Ni (3 to 26 ppm) and Zn (12 to 136 ppm). Very low concentrations of Ti (<100 ppm), Cr(< 100 ppm) and V (Avg 7.8 ppm) were also detected in the studied samples. Average total value for REE in the magnetite ores are ΣREE 27.88, (Eu/Sm) 0.309, (Sm/Yb) 10.32 and (La/Lu) 104.14.

The Fe2O3 value of the host rocks ranges from 12.02 to 14.1 wt% and MgO ranges from 9.2 to 9.32 wt% and Al2O3 varies from 13.6 to 17.3 wt%. The K2O values of the host rocks range widely from 1.12 to 1.60 wt%. In the AFM diagram (Jensen, 1976, Fig. 2) the rocks fall in the high Fe-tholeiite basalt field.

The SiO2 content varies between 43.7 and 44.80 wt% and average concentrations of Co 50.933ppm, Ni 29.333 ppm, Cr 100 ppm, ΣLREE 98.64 and ΣHREE 16.59 were present in the host rock. The concentration of Ti in these rocks is very low (maximum 22.309 ppm). Enrichment in Light Rare Earth Elements (LREEs) is observed relative to the Heavy Rare Earth Elements (HREEs) on normalized spider diagram of REEs (Fig.3).

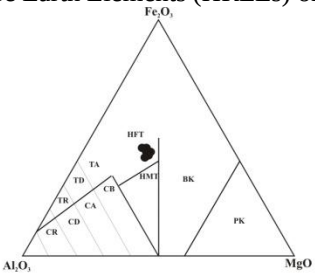

Fig.2: Rock classification after Jensen(1976), PK= Peridotitic Komatiite BK= Basaltic Komatiite, HFT= High Iron Tholeiite, HMT- High Magnesium Tholeiite, TA= Tholeiite Adesite, TD= Tholeiite Dacite, TR= Tholeiite Rhyolite CA= Calc Alkaline Adesite, CR= Calc Alkaline Rhyolite, CD= Calc Alkaline Dacite, CB= Calc Alkaline Basalt.

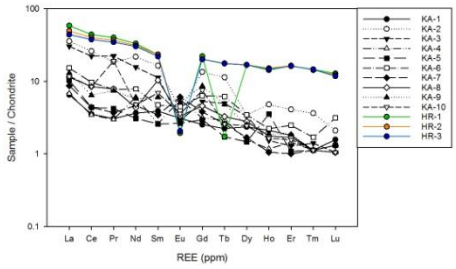

Fig 3: REE normalized spider diagram

VII. DISCUSSION

The high concentration of iron oxides in the mineralized zones shows that the oxygen fugacity (fO2) must have been sufficient for magnetite mineralization. Ore crystallization began initially with the formation of massive magnetite during high oxygen fugacity conditions. The fO2 decreased as much of the iron oxidized to form the isotropic, very pale pinkish to brownish gray magnetite (Gates, 2014). This oxidizing effect is demonstrated by the formation of hematite at the expenses of martite. Similar observations have been reported by other authors (Rosiere and Rios., 2004; Nold et al., 2013). The formation of sulfide minerals belongs to the latest hydrothermal alteration stage.

High Mn concentration in some iron ore samples can be attributed to the high activity of this metal in the mineralizing fluid but the absence of Mn minerals in the studied ore samples indicates that Mn2+ preferentially substituted for Fe2+ in magnetite lattice. High variation in Fe2O3 content of the ores over short distances across the ore body is consistent with the hydrothermal mode of ore formation. The absence of skarn type minerals such as garnet, wollastonite and pyroxene, indicates that iron mineralization in the study area occurred during fluid circulation, unlike those involved in skarn iron deposits (Mei et al., 2015).

Cobalt and Ni with similar ionic radii to Fe2+ substitute for iron in magnetite lattice. Due to the low concentration of Co and Ni cobaltite, safflorite, danite and niccolite are absent from the iron ores. High Co/Ni ratio of the iron ores (average 3.9) and Cr/V (avg 17.67) imply a typical hydrothermal origin for magnetite in the present deposit (Li et al., 2015). In contrast, a magmatic origin of the present deposit is excluded by the very low V, Ti and P contents in the iron ores. On the other hand V concentration of the present ore deposit, like other hydrothermal iron deposits, is very low (average 7.8 ppm). Cr concentration of the iron ore samples from the study area (<100 ppm) implies a hydrothermal origin for the studied ores.The low Ga concentration (average 3.3 ppm) in the present ore deposit is

also consistent with the hydrothermal origin of magnetite (Knipping et al., 2015).The chondrite normalized REE distribution pattern in the present iron ores are similar to those of other hydrothermal deposits (e.g. Iron Springs in USA and Igarape Bahia in Brazil) which is marked by positive Eu and negative Ce anomalies. The Eu/Sm, Sm/Yb , La/Lu , LREE/ HREE ratios also characterize the hydrothermal origin of the present iron deposit. The similarity of REE distribution patterns of igneous rocks and ore samples indicates the role of igneous activity in mineralization system (Fig.3). High iron content in the host may be regarded as the source of iron and heat in the mineralizing system. Relatively low sulfur activity in ore bearing fluid from the present deposit is indicated by the general paucity of sulfide minerals in the ore bodies. An increase in pH of the mineralizing fluid induced chalcopyrite and pyrite precipitation (Skirrow and Walshe., 2002).There are some similarities between the present magnetite ores and other hydrothermal Fe-oxide deposits worldwide, such as the Andean iron oxides and the Iron springs deposit from Utah (Sillitoe., 2003).

VIII. REFERENCES

[1] Nadoll, P., Mauk, J. L., Hayes, T.S., Koenig, A.E., Box, S.E., (2012). Geochemistry of magnetite from hydrothermal ore deposits and host rocks of the Mesoproterozoic Belt Supergroup, United states. Econ. Geol. 107, 1275-1292.

[2] Dar, S.A.S., Bares, S. J., Beaudoin, G., Meric, J., Boutroy, E., Potvin- Doucet, C., (2014).Trace elements in magnetite as petrogenetic indicators. Miner. Deposita, 1-12.

[3] Nadoll, P, Angerer, T., Mauk, J.L., French, D., Walshe, J., (2014). The chemistry of hydrothermal magnetite: a review ore Geol. Rev. 61, 1-32.

[4] Chen,W.T., Zhou, M-F., Li,X., Gao. J-F., Hou, K., (2015b). In- situ LA-ICP-MS trace elemental analyses of magnetite: Cu-(Au, Fe) deposits in the Khetri copper belt in Rajasthan Province. NW India. Ore Geol. Rev. 65, 929-939.

[5] Verma, R.K., (1985). Gravity field, seismicity and tectonics of the Indian Peninsula and the Himalayas. Allied Publishers Private Limited, New Delhi. 213 pp.

[6] Sharma, R.S. (2009). Cratons and Fold belts of India. Springer-Verlag Publ. Berlin 304p.

[7] Patel, S.C., Sundararaman, S. Dey, R., Thakur, S.S. and Kumar, M., (2007). Deformation pattern in a Proterozoic low pressure metamorphic belt near Ramanujganj, Western Chotanagpur Terrain. Jour Geol. Soc. India, 70, 207-216.

[8] Satyanarayanan, M., Balaram, V., Sawant, S.S., Subramanyam, K.S.V., Vamsi Krishna, G., Dasaram, B., and Manikyamba, C., (2018). Rapid determination of REEs, PGEs, and other Trace element in geological and environmental materials by High Resolution Inductively Coupled Plasma Mass Spectrometry. Atomic Spectroscopy. 39(1), 1-15.

[9] Jensen, L.S., (1976). A New cation plot for classifying subalkalic volcanic Rocks: Publications of the Ontario Division of Mines, Toronto,Ontario. 22p.

[10] Kalczynski, M. J., Gates, A. E., (2014). Hydrothermal alteration, mass transfer and magnetite mineralization in dextral shear zones, Western Hudson Highlands, New York, United states. Ore Geol. Rev. 61, 226-247.

[11] Rossier, C.A., Rios, F.J., 2004. The origin of hematite in high grade iron ore based on infra-red microscopy and fluid inclusion studied: the example of the Conceicao mine, Ouadrilatero. Brazil. Econ. Geol. 99, 611-624.

[12] Nold, J. L., Davidson, P., Dudley, M. A., (2013). The Pilot knob magnetite deposit in the Proterozoic St. Francois Mountains terrane, southeast Missouri, USA: a magmatic and hydrothermal replacement iron deposit. Ore Geol. Rev. 53, 446-469.

[13] Mei, W., Lu, X., Cao, X., Liu, Z., Zhao, Y., Al, Z., Tang, R., Abfaua, M.M., (2015). Ore genesis and hydrothermal evolution of the Huanggang skarn iron-tin polymetallic deposit, southern Great Xing'an range: evidence from fluid inclusions and isotope analyses. Ore Geol. Rev. 64, 239-252.

[14] Li, S., Yang, X., Sun, W., (2015). The Lamandau IOCG deposit, southwestern Kalimantan Island Indonesia: evidence for its formation from geochronology, mineralogy and petrogenesis of igneous host rocks. Ore Geol. Rev. 68. 43-58.

[15] Knipping, J.L., Bilenker, L.D., Simon, A.C., Reich, M., Barra, F., Deditius, A.P., Walle, M., Heinrich, C.A., Holtz, F., Munizaga, R.,(2015). Trace elements in magnetite from massive iron oxide-apatite deposits indicate a combined formation by igneous and magmatic-hydrothermal processes. Geochim. Cosmochim. Acta 171, 15-38.

[16] Skirrow, R.G., Walshe, J.L., (2002). Reduced and oxidized Au-Cu-Bi iron oxide deposits of the Tennant Creek inlier, Australia: an integrated geologic and chemical model. Econ. Geol. 97, 1167-1202.

[17] Sillitoe, R.H., (2003). Iron oxide-copper-Gold deposits: an Andean view. Miner. Deposita 38, 787-812.